The Structure of β-Keratin

R. D. B. FRASER, T. P. MACRAE, D. A. D. PARRY and E. SUZUKI

The structure of β-keratin has been re-investigated. A trial structure obtained from energy calculations was refined on the basis of quantitative X-ray diffraction and infra-red data. If a crystal model with inter-sheet packing disorder similar to that present in the β-form of poly-L-alanine is assumed, the observed data can be satisfactorily accounted for by an antiparallel chain pleated sheet conformation. An alternative model with intra-sheet disorder was also considered. A Fourier synthesis using the observed hk0 intensities and calculated phases yielded an electron density map in which the main chain atoms were clearly resolved.

STUDIES of the X-ray diffraction patterns of *Bombyx mori* silk fibroin[1], *Chrysopa flava* silk[2] and the β-form of poly-L-alanine[3] provide strong support for the existence of the antiparallel chain pleated sheet structure[4] in these materials. It seems likely that a pleated sheet structure is also present in β-keratin but so far it has not proved possible to establish whether the arrangement of the chains within the sheets is parallel, antiparallel or random.

Astbury and coworkers[5,6] indexed their X-ray data obtained from β-keratin on a two-chain cell and interpreted this as indicating an antiparallel arrangement of chains linked through hydrogen bonds in the manner illustrated in *Figure 1*(a). Pauling and Corey[4], on the other hand, considered that the axial repeat of the structure, which is shorter than that in silk fibroin and in poly-L-alanine, indicated a parallel arrangement of chains as in *Figure 1*(b). Miyazawa and Blout[7] claimed that the fine structure of the Amide I band in the infra-red spectrum supported this conclusion.

Subsequently Fraser and MacRae[8] reported that X-ray reflections had been detected at spacings which could not be explained by a parallel chain arrangement and Bradbury and Elliott[9] detected an Amide I component in the infra-red spectrum of stretched horse hair at a frequency characteristic of the antiparallel arrangement.

The present communication describes a re-investigation of this problem in which quantitative X-ray and infra-red data were collected and analysed with a view to determining the nature of the chain arrangement in β-keratin.

EXPERIMENTAL

Specimens of quill from the porcupine *Hystrix cristata* approximately $10 \times 2 \times 0{\cdot}3$ mm were stretched in steam to about 75% extension over a period of 5-6 h and held at this extension in steam for a further 2 h.

For X-ray examination the specimens were mounted with the smallest dimension parallel to the beam and the diffraction pattern recorded with a multiple film pack in a Unicam 3 cm cylindrical camera. Nickel filtered copper radiation was used and dry helium was circulated through the camera during the exposure. Integrated intensities were measured with a Joyce

Loebl microdensitometer by recording the optical density in two traces through the maximum of each arc in the fibre pattern. The first trace was taken tangentially along the arc, the second perpendicular to this direction. After correction for background, the integrated intensity was taken as the product of the two areas divided by the peak height[10].

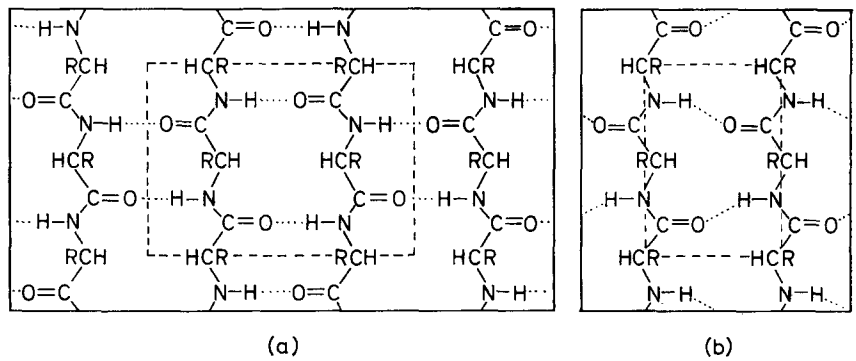

(a) (b)

Figure 1—Hydrogen bonding arrangement in (a) the antiparallel chain pleated sheet and (b) the parallel chain pleated sheet

Specimens suitable for infra-red studies were prepared by cutting uniform sections about 2μ in thickness from the specimens prepared for X-ray studies. The technique of section cutting and mounting has been described elsewhere[11]. A Beckman IR-9 prism/grating spectrophotometer equipped with twin beam condensers and a selenium polarizer[12] was used to obtain spectra with the electric vector vibrating first parallel then perpendicular to the fibre axis. The dichroism curve in the Amide I region was analysed by an iterative non-linear least-squares procedure[13] assuming that each component could be represented by a linear combination of Gauss and Cauchy functions in the ratio f to $(1-f)$ having the general formula

$$\Delta D/\Delta D_m = f \exp\{-\ln 2\,[2(\nu-\nu_m)/\Delta\nu_{1/2}]^2\} + (1-f)/\{1+[2(\nu-\nu_m)/\Delta\nu_{1/2}]^2\} \quad (1)$$

where ΔD is the contribution of the component to the dichroism at frequency ν, ΔD_m and ν_m specify the peak height and its frequency and $\Delta\nu_{1/2}$ is the width of the component at half peak height.

DERIVATION OF TRIAL STRUCTURE

A difficulty in attempting to use diffraction data from fibre patterns for structure determination is the paucity of data in relation to the number of parameters required to specify the structure. In order to reduce the number of independent parameters advantage may be taken of the known stereochemistry of the polypeptide chain[14] and of the possibility of calculating the interaction energy of different packing arrangements[15,16]. If a trial structure sufficiently close to the actual one can be derived from such considerations, the possibility arises of using a least-squares refinement technique to opti-

mize the structural parameters even though the number of data is considerably smaller than usually required for this method.

In the present instance a trial structure was derived by generating a chain conformation having the observed axial repeat and then computing the packing energy of the pleated sheet structure for various dispositions of the chain within the unit cell.

Table 1. Atomic coordinates of a polypeptide chain with axial repeat $b=6{\cdot}68$Å having the standard peptide geometry[17] and $\tau[NC^{\alpha}C']=109{\cdot}47°$

Atom	*u*(Å)	*v*(Å)	*w*(Å)
C^{α}	0	0	0·907
H^{α}	−1·093	0·099	0·981
N	0·332	−1·234	0·180
H	1·303	−1·329	−0·038
C′	0·572	1·204	0·155
O	1·783	1·284	−0·096
C^{β}	0·603	−0·058	2·312

Equivalent positions u, v, w; $-u, v+3{\cdot}34$Å, $-w$.

The coordinates of a polypeptide chain having the standard peptide group geometry[17], $\tau[NC^{\alpha}C']=109{\cdot}47°$ and an axial repeat, *b*, of 6·68Å were generated and are given in *Table 1*. The coordinate system *Ouvw*, shown in *Figure 2*(a), was chosen so that the chain axis coincides with *Ov* and C^{α} lies on *Ow*. All possible antiparallel chain pleated sheet structures may then be generated by rotating the chain through an angle α about *Ov*, displacing it a distance δ parallel to *Ov* and setting the origin *O* at a position $(a/4, 0, 0)$ in the unit cell with *Ou* parallel to the *a* axis and *Ov* parallel to the *b* axis. The positions of all other chains in the sheet are then fixed by symmetry (*Figure 2*(b)).

In the energy calculations, terms corresponding to van der Waals, electrostatic, and hydrogen bonding interactions were included together with the rotational potential around single bonds. Details of the expressions used and the methods of computation have been described elsewhere[18]. The interaction energy depends on the nature of the side chain and on its conformation. For the present purposes an 'average' side chain $—CH_2—CH_3$ was used. The effect of varying the rotational angle χ_{12} about the $C^{\alpha}C^{\beta}$ bond, the inter-chain distance $(a/2)$ and the parameters α and δ were explored in a systematic manner. The chain arrangement with minimum energy was found to occur with $\chi_{12}=300°$, $a=9{\cdot}4$Å, $\alpha=-18°$ and $\delta=0{\cdot}1$Å, and these values were used to generate the trial structure. The value of *a* derived in this manner is consistent with the observed spacing of the 200 reflection, and the dependence of interaction energy on α and δ for $a=9{\cdot}4$Å in the vicinity of the minimum energy conformation is illustrated in *Figure 3*. The interaction map for a CH_3 side chain was also calculated and had many features in common with that shown in *Figure 3*. A sharp rise in energy for α values outside the range $-22°$ to $-5°$ was present in both instances and may be attributed to the close approach of the β-carbon atoms in adjacent chains.

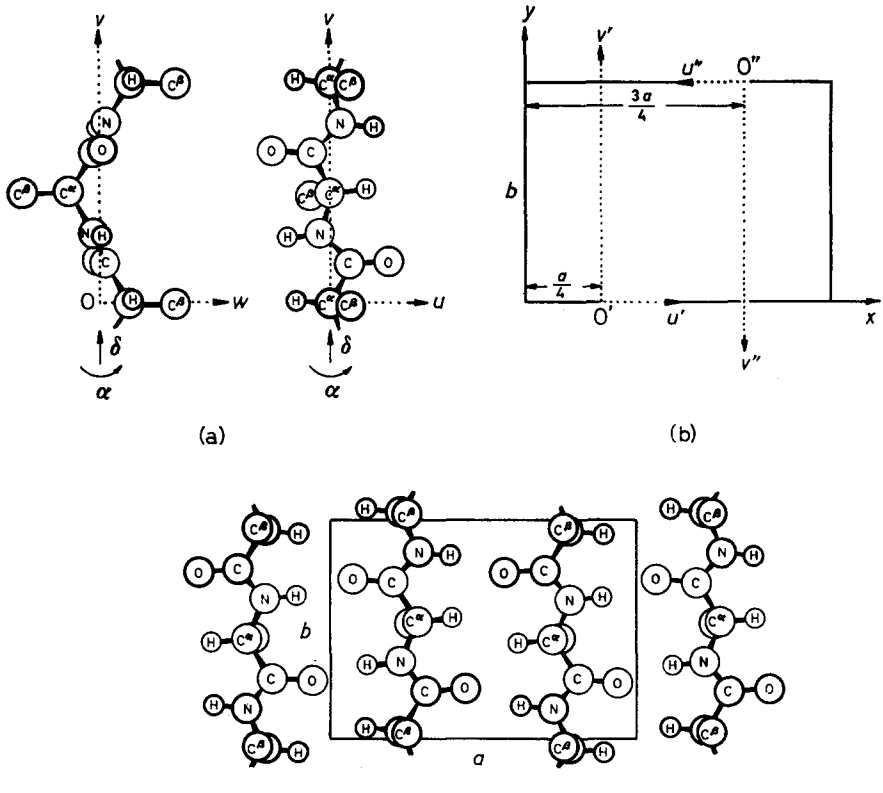

Figure 2—(a) u and w axis projections of a polypeptide chain having the atomic co-ordinates given in *Table 1*. (b) The repeating unit of the antiparallel chain pleated sheet which may be generated by setting one chain at $O'u'v'w'$ and another inverted chain at $O''u''v''w''$. Any packing arrangement may be generated by applying an appropriate displacement δ parallel to Ov and rotation around Ov to the chain depicted in (a). (c) In the case illustrated $\delta = 0{\cdot}28$Å and $\alpha = -16°$

CALCULATION OF X-RAY PATTERN

For the purposes of least squares refinement it is convenient to formulate the expression for the calculated intensity in terms of the structure factor of a chain referred to the coordinate system $Ouvw$ shown in *Figure 2*(a) for some given value of α and with $\delta = 0$. If the value of this structure factor in the a^*b^* plane is denoted by

$$F_\alpha(hk0) = A_\alpha(hk0) + iB_\alpha(hk0) \tag{2}$$

the structure factor for a chain displaced by distance δ parallel to Ov is

$$F_{\alpha\delta}(hk0) = F_\alpha(hk0) \exp(2\pi ik\delta/b). \tag{3}$$

The structure factor for the pleated sheet, referred to the origin of the unit cell (*Figure 2*(b)) is then

$$F(hk0) = F_{\alpha\delta}(hk0) \exp(2\pi ih/4) + F^*_{\alpha\delta}(hk0) \exp(2\pi i \times 3h/4) \tag{4}$$

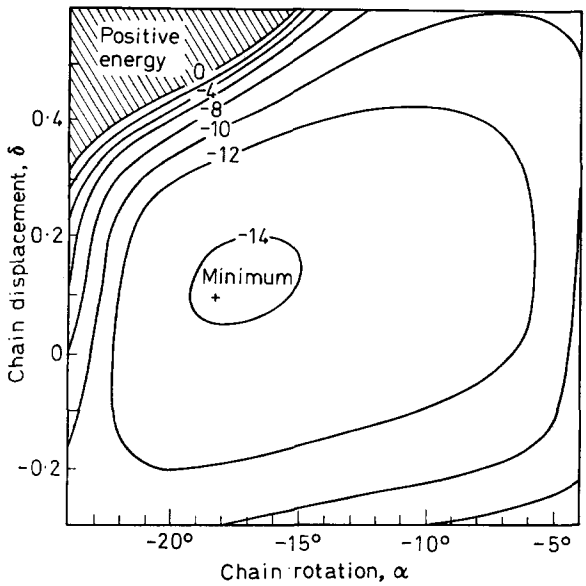

Figure 3—Portion of the energy map for β-keratin showing the effect of the parameters α and δ on the lattice energy per residue in the antiparallel chain pleated sheet. Outside the range of α illustrated the energy increases sharply due to the close approach of the β-carbon atoms in adjacent chains. Contour interval 2 kcal/mole

The first term represents a chain displaced $a/4$ from the reference point for phase and the second an inverted chain displaced by $3a/4$; $F^*_{a\delta}$ indicates the complex conjugate of $F_{a\delta}$. Substituting (3) in (4) and separating real and imaginary parts we obtain for h even,

$$A(hk0) = 2[A_a(hk0)\cos(2\pi k\delta/b) - B_a(hk0)\sin(2\pi k\delta/b)] \quad (5)$$

$$B(hk0) = 0 \quad (6)$$

and for h odd,

$$A(hk0) = 0 \quad (7)$$

$$B(hk0) = 2[A_a(hk0)\sin(2\pi k\delta/b) + B_a(hk0)\cos(2\pi k\delta/b)] \quad (8)$$

In order to compare the calculated diffraction pattern with the observed integrated intensities allowance must be made for Lorentz, polarization and temperature factors and a correction term of the form

$$C(hk0) = \kappa \exp\{-\tfrac{1}{2}(\mathrm{B}_x h^2/a^2 + \mathrm{B}_y k^2/b^2)\}/LP \quad (9)$$

was used to modify the calculated values. The constant κ is used to match the arbitrary observed intensity scale, B_x and B_y are temperature factor components and L and P are the Lorentz and polarization factors given by Arnott[19].

The intensities calculated using equations (5) to (9) are appropriate to the a^*b^* plane of the reciprocal lattice for a single sheet or for an ortho-

rhombic packing arrangement. These values will be modified by imperfections in sheet packing and by the presence of any wrongly directed chains.

Imperfections in sheet packing

The very diffuse nature of the reflections with $l \neq 0$ indicates that the crystallites in β-keratin are very poorly developed in a direction perpendicular to the plane of the pleated sheet[8]. A crude estimate of the average number of sheets in a crystallite ($\overline{M}$) may be obtained from the breadth of the 001 reflection. The observed value of 0·046Å^{-1} indicates that the average dimension of the crystallites perpendicular to the sheet is approximately $(0{\cdot}046)^{-1} = 22$Å and as the inter-sheet distance is 9·7Å[8], $\overline{M}$ probably lies between 2 and 3.

If the sheets are packed in perfect register the calculated integrated intensity of the $hk0$ reflections is simply

$$I_c(hk0) = C(hk0)\, B^2(hk0) \text{ for odd } h \tag{10}$$

$$I_c(hk0) = C(hk0)\, A^2(hk0) \text{ for even } h \tag{11}$$

but if a random displacement of $\pm a/2$ occurs between adjacent sheets as in the β-form of poly-L-alanine[3] the reflections with odd h are reduced in intensity by a factor $1/\overline{M}$ (Appendix 1). Thus

$$\begin{aligned} I_c(hk0) &= C(hk0)\, B^2(hk0)/\overline{M} \quad \text{for odd } h \\ I_c(hk0) &= C(hk0)\, A^2(hk0) \qquad\quad \text{for even } h \end{aligned} \tag{12}$$

Imperfections within a sheet

If the alternation of chain direction within a sheet is imperfect the effect will be somewhat similar to imperfections in sheet packing in that the reflections with odd h will be reduced in intensity by a constant factor. This factor $\gamma(N, p)$ is a function of the number of chains in a sheet (N) and the probability p that any particular chain is correctly directed with respect to the preceding one. The function $\gamma(N, p)$ is derived in Appendix 2 where it is shown that

$$I_c(hk0) = C(hk0)\gamma(N, p)B^2(hk0) \qquad \text{for odd } h \tag{14}$$

and

$$I_c(hk0) = C(hk0)[A^2(hk0) + 4\gamma(N, 1-p)\,.\, B^2_{a\delta}(hk0)] \text{ for even } h \tag{15}$$

The measured breadth of the 200 reflection is 0·021Å^{-1} and the mean value of N is therefore approximately equal to $(0{\cdot}021 \times a/2)^{-1} = 10{\cdot}1$. The function $\gamma(10, p)$ is illustrated in *Figure 4*.

REFINEMENT OF MODEL

An iterative non-linear least-squares refinement of the trial structure was carried out on the basis of the observed X-ray data for perfect orthogonal packing, for inter-sheet disorder with $\overline{M} = 2$ and 3 and for intra-sheet dis-

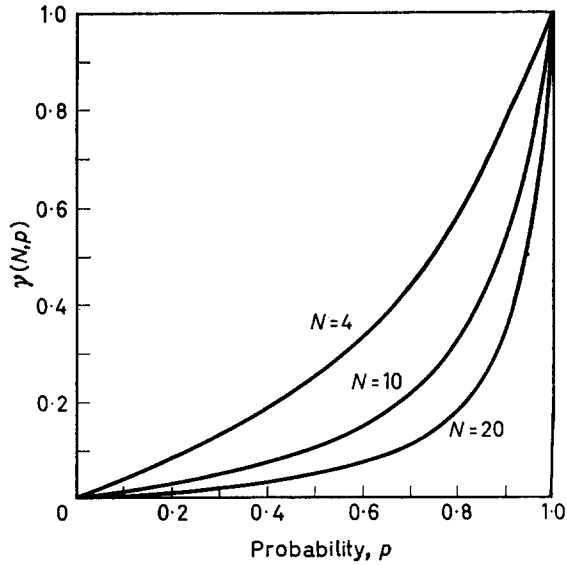

Figure 4—The function $\gamma(N, p)$ derived in Appendix 2 for $N=4$, 10 and 20. As N increases further γ becomes vanishingly small unless p is very close to 1

order, and the results are summarized in *Table 2*. The goodness of fit was measured by means of a normalized weighted standard deviation

$$R = \left\{ \sum W(hk0)[I_o(hk0) - I_c(hk0)]^2 / \sum W(hk0) I_o^2(hk0) \right\}^{1/2}. \quad (16)$$

where $W(hk0)$ is a weighting function and $I_o(hk0)$ is the observed integrated intensity. As the proportional error was approximately constant for the medium and strong reflections, W was taken as $1/I_o$ for $I > 5I_{min}$, where I_{min} was the minimum observable intensity. For $I \leqslant 5I_{min}$, W was taken as $1/5I_{min}$. Unobserved reflections were allotted an intensity equal to $0{\cdot}5I_{min}$. The 020 meridional reflection was not included as it could not be scaled with any certainty[19].

A preliminary survey showed that acceptable R values could only be obtained if the contribution of the γ-carbon atoms was omitted. This indicates that the position of these atoms, when present, must be highly variable. The significance of the R factor in relation to the number of observed data and the number of parameters can be tested by a procedure described by Hamilton[20]. An analysis of the R factors in *Table 2* by this procedure reveals that the positions of the β-carbon atoms, when present, must be subject to considerably greater displacements from their mean positions than the main chain atoms as the R factor is significantly lower when their contribution is omitted. However, the number of data is insufficient to refine a combined temperature and disorder factor for each atom.

The lowest R factors are obtained for the models with either intra- or inter-sheet disorder. These models involve an extra parameter compared

Table 2. Summary of results obtained from least squares refinement of minimum energy structure ($\alpha_0 = -18°$, $\delta_0 = 0{\cdot}1$Å) on the basis of the X-ray diffraction data. R is the normalized weighted standard deviation

Chain rotation (deg.)	*Orthogonal packing*		*Inter-sheet disorder*				*Intra-sheet disorder*		
			$\overline{M}=2$		$\overline{M}=3$				
	δ(Å)	R	δ(Å)	R	δ(Å)	R	δ(Å)	p*	R
Main chain									
α_0-20	0·27	0·398	0·26	0·380	0·24	0·380	0·26	0·87	0·830
-15	0·31	0·334	0·28	0·319	0·26	0·321	0·28	0·87	0·321
-10	0·32	0·256	0·29	0·240	0·27	0·242	0·29	0·87	0·239
-5	0·32	0·191	0·29	0·170	0·27	0·171	0·29	0·87	0·168
α_0	0·32	0·166	0·30	0·136	0·27	0·136	0·28	0·84	0·135
α_0+5	0·33	0·169	0·30	0·138	0·27	0·136	0·27	0·81	0·135
$+10$	0·33	0·182	0·30	0·150	0·27	0·147	0·00	0·33	0·145
$+15$	0·34	0·206	0·30	0·163	0·28	0·155	−0·03	0·18	0·194
$+20$	0·35	0·243	0·32	0·173	0·29	0·156	−0·03	0·25	0·129
Main chain + C^β									
α_0-20	0·13	0·846	*0·21*	*0·619*†	0·21	0·535	−0·03	0·21	0·411
-15	x	x‡	0·26	0·509	0·23	0·462	x	x	x
-10	x	x	*0·27*	*0·350*	0·24	0·327	x	x	x
-5	x	x	0·28	0·295	0·24	0·289	0·04	0·25	0·290
α_0	0·33	0·344	0·29	0·348	0·27	0·352	x	x	x
α_0+5	0·34	0·383	0·33	0·393	0·98	0·568	*0·39*	*1·22*	*0·370*
$+10$	0·76	0·434	0·72	0·323	*0·75*	*0·311*	*0·73*	*0·83*	*0·309*
$+15$	0·59	0·406	0·63	0·334	0·68	0·315	*1·18*	*−0·18*	*0·908*
$+20$	0·68	0·508	0·62	0·412	*0·62*	*0·372*	*0·28*	*0·14*	*0·300*

*Assuming $N=10$.

†Italics indicate one or more parameters have unreasonable values, e.g. B_x, B_y or $p<0$.

‡x indicates no solution, i.e. refinement diverges.

with the orthogonally packed model but comparison of R factors by Hamilton's procedure reveals that both are significantly better at the 1·7% level. The difference in R factors between the intra- and inter-sheet disorder models is not significant, however, even at the 50% level.

The R factor proved to be very sensitive to the parameter δ but relatively insensitive to α. The insensitivity to chain rotation, illustrated in *Figure 5* is readily understood as the projection of the sheet onto the *ab* plane is only slightly affected by changes in α. In order to obtain a more precise estimate of α additional evidence from infra-red measurements and energy calculations was required.

INTERPRETATION OF INFRA-RED DATA

In the antiparallel chain pleated sheet structure the interaction between the four amide groups in the unit cell leads to a splitting of the Amide I vibration into four components. Three of these, designated $\nu_\perp(\pi, 0)$, $\nu_{/\!/}(0, \pi)$ and $\nu_\perp(\pi, \pi)$, are infra-red active and have transition moments parallel to the *a*, *b* and *c* axes respectively. The magnitudes of the transition moments will be proportional to the components T_x, T_y and T_z of the transition moment associated with the unperturbed Amide I mode of an individual amide group. These considerations are unlikely to be affected by inter-sheet

packing faults but intra-sheet disorder would destroy the regular coupling between oppositely directed chains and unless $p \simeq 1$ the Amide I mode would not be split into components.

The detailed analysis of the observed spectrum of β-keratin will be discussed elsewhere[22] but the feature of importance to the present investigation

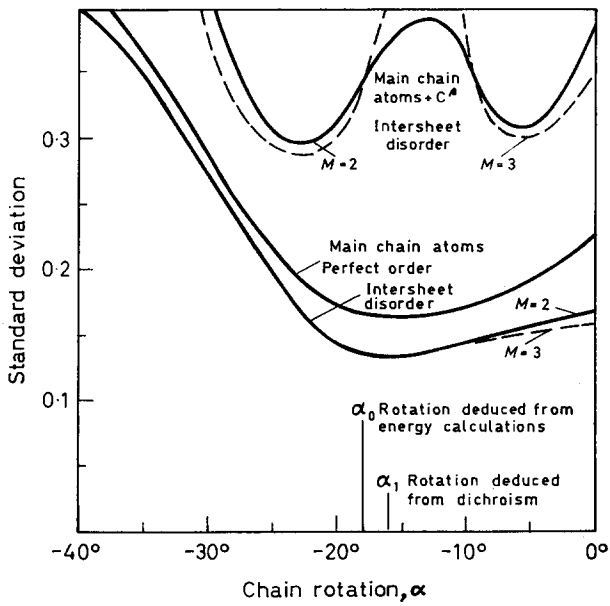

Figure 5—Comparison of normalized, weighted standard deviation (R) between observed and calculated X-ray intensities for various models. The values of α deduced from infra-red dichroism (α_1) and from energy calculations (α_0) are indicated

is that the ratios of the intensities of the three infra-red active Amide I components provide information about the likely value of the parameter α for the orthogonal model and for the model with inter-sheet disorder.

The analysis of the observed dichroism is shown in *Figure 6* and it will be seen that a close fit to the observed data can be obtained by including an Amide II component at 1 527 cm^{-1} and Amide I components at 1 629, 1 657, 1 683 and 1 697 cm^{-1}. The components at 1 629, 1 683 and 1 697 cm^{-1} have relative intensities, dichroisms and frequencies of the order expected for an antiparallel chain pleated sheet whilst the component at 1 657 cm^{-1}, with parallel dichroism, may be attributed to residual α-material.

The orientation of the transition moment in the plane of the amide group for the unperturbed Amide I mode can be calculated from the ratio of the integrated dichroism component associated with $\nu_{//}(0, \pi)$, $\Delta D_{0\pi}$, to the sum of the perpendicular components $\Delta D_{\pi 0}$ and $\Delta D_{\pi\pi}$. The orientation so deduced is identical with that found in silk fibroin[11] and thus sufficient reliance can be placed on the analysis to warrant using the data to estimate the value of α.

The components of the transition moment associated with the unperturbed Amide I mode of an individual amide group, T_u, T_v and T_w parallel to *Ou*, *Ov* and *Ow* respectively, can be calculated for the standard conformation given in *Table 1*, and the integrated intensities of the perpendicular components of the dichroism, $\Delta D_{\pi 0}$ and $\Delta D_{\pi\pi}$, will be proportional to

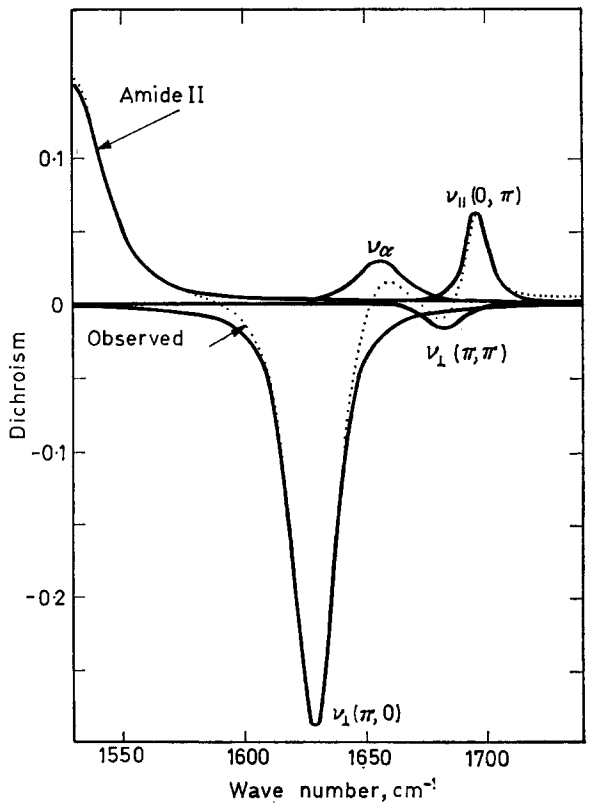

Figure 6—Analysis of dichroism in Amide I region of the infra-red spectrum of β-keratin. The curve obtained by adding the resolved components together with a sloping linear baseline (not shown) reproduce the observed curve (shown dotted) to within experimental error

$\frac{1}{2}[T_u \cos\alpha - T_w \sin\alpha]^2$ and $\frac{1}{2}[T_u \sin\alpha + T_w \cos\alpha]^2$ respectively.

Thus the chain rotation α may be estimated from the ratio $\Delta D_{\pi 0}/\Delta D_{\pi\pi}$ by means of the expression

$$\alpha = -\tan^{-1}(T_u/T_w) \pm \tan^{-1}(\Delta D_{\pi 0}/\Delta D_{\pi\pi})^{1/2} \qquad (17)$$

Taking the observed value of $\Delta D_{\pi 0}/\Delta D_{\pi\pi}$ (=18·1) and the calculated value of T_u/T_w (= −23·6) we obtain $\alpha = -16°$ (α_1) or $\alpha = 11°$ (α_2).

DISCUSSION

The difference in R factors for the models with inter- and intra-sheet disorder (*Table 2*) are not significant and both must be considered as possibilities.

A value of 0·129 for R was achieved with $\alpha = +2°$ and $p = 0·25$ for the model with intra-sheet disorder but the energy is high and the value of p is so low that the structure is more nearly a parallel-chain pleated sheet, which is not consistent with the infra-red data. The value of 0·135 for R achieved with $\alpha = -18°$ and $p = 0·84$ indicates that the model with intra-sheet disorder provides a satisfactory explanation of the X-ray data with a conformation which is close to the minimum energy conformation. A likely consequence of intra-sheet disorder would be a broadening of the reflections with odd h and an imperfect resolution of the Amide I components in the infra-red spectrum. No evidence of either of these effects could be found but until the magnitudes of these effects for $p = 0·84$ can be quantitatively predicted the possibility of intra-sheet disorder cannot be entirely eliminated.

As regards the model with inter-sheet disorder similar to that found in poly-L-alanine[3] the two values $\alpha_1 = -16°$ and $\alpha_2 = 11°$ deduced from the infra-red data can be distinguished on the basis of the energy calculations which indicate a pronounced minimum at $\alpha = -18°$ and a sharp rise outside the range $-22°$ to $-5°$. The R factor for this model with $\overline{M} = 2$ or 3 is also a minimum in the vicinity of α_1 and it is thus consistent with all the observed data.

A final least squares refinement in which the value of α was fixed at $\alpha_1 = -16°$ and the parameter $\overline{M}$ released gave an R factor of 0·133 and optimized values of $\delta = 0·28$Å, $B_x = 5·5$Å^{-2}, $B_y = 10·4$Å^{-2}, $\kappa = 0·0137$, and $\overline{M} = 2·6$. This structure is illustrated in *Figure 2*(c), the atomic coordinates are given in *Table 3* and the observed and calculated intensities are compared in *Table 4*.

Table 3. Atomic coordinates for the asymmetric unit of the antiparallel chain pleated sheet* in β-keratin refined on the basis of X-ray diffraction and infra-red data

Atom	*x*(Å)	*y*(Å)	*z*(Å)
C	2·100	0·280	0·872
N	2·619	−0·954	0·264
H	3·613	−1·049	0·323
C′	2·857	1·484	0·307
O	4·091	1·564	0·400
H	1·029	0·379	0·641

*Equivalent positions x, y, z; $4·7-x, 3·34+y, -z$; $9·4-x, -y, z$; $4·70+x, 3·34-y, -z$.

FOURIER SYNTHESIS

The phases given in *Table 4* can be used in conjunction with the observed intensities, suitably corrected for Lorentz and polarization factors, to obtain an electron density map of the β-keratin structure projected parallel to the c axis. To allow for the effects of inter-sheet disorder the intensities of the reflections with odd h were multiplied by the optimized value of $\overline{M} = 2·6$ as required by equation (12). The map so obtained is shown in *Figure 7* and the zigzag polypeptide chain can be seen and the oxygen atom is clearly resolved. No evidence of electron density due to the side chains is apparent.

Additional resolution was obtained by using the technique of artificial sharpening in which the observed structure amplitudes were multiplied by a term

$$\exp\left[\tfrac{1}{4}(B_x h^2/a^2 + B_y k^2/b^2)\right] \qquad (14)$$

where B_x and B_y had the optimized values of 5·5 and 10·4Å^2 respectively. In the sharpened map, shown in *Figure 8*, electron density peaks in the positions expected for the C^α, N and C′ atoms are just resolved.

Table 4. Comparison of observed intensities with those calculated for the structure given in *Table 3* with inter-sheet disorder

hk	*Integrated intensity*		*Observed structure amplitude*	*Calculated phase (radian)*
	Observed I_o	*Calculated* I_c	F_o	
20	100*	103†	35·3‡	π
40	9	12	16·5	0
60	4	3	14·4	π
11	0	0	—	—
21	30	26	20·8	0
31	0	0	—	—
41	8	7	16·8	0
51	0	0	—	—
61	0	0	—	—
12	0	1	—	—
22	10	7	13·1	π
32	0	1	—	—
42	0	0	—	—
52	0	0	—	—
62	0	0	—	—
13	3	3	9·5	0
23	13	15	17·3	π
33	2	1	12·4	π
43	0	0	—	—
53	0	0	—	—
63	1	1	11·5	π

*Zero in this column indicates below minimum observable intensity.

†Zero in this column indicates $I_c < 0{\cdot}5$.

‡Corrected for Lorentz, polarization and temperature factors (see text).

Finally a Fourier synthesis was performed using the differences between the observed and calculated structure amplitudes in conjunction with the calculated phases. The electron density map consisted of very weak pairs of positive and negative maxima in the vicinity of the main chain atoms. The separation of the peaks indicated that the atomic positions given in *Table 3* might be in error by approximately 0·1 to 0·2Å but the number of data available is insufficient to attempt refinement of individual atomic positions. The most likely cause of these errors is that the actual values of the bond angles in the main chain differ slightly from the standard values used to generate the atomic coordinates given in *Table 1*.

No significant peaks appeared near the positions anticipated for the β- or γ-carbon atoms.

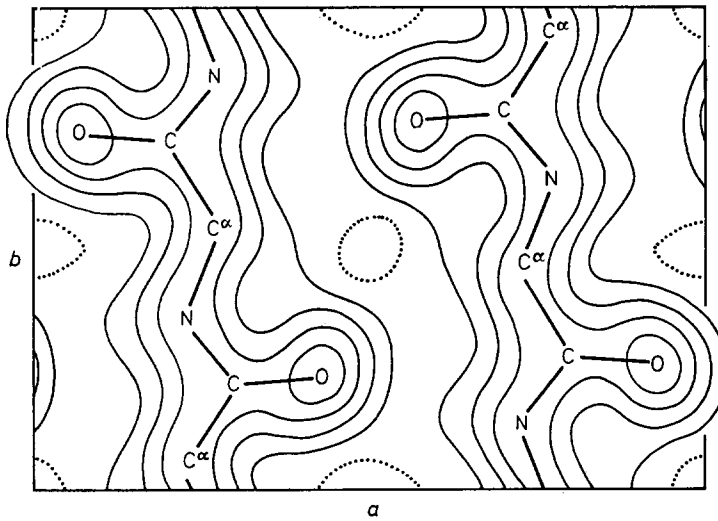

Figure 7—Electron density map of β-keratin obtained by Fourier synthesis using the observed intensities in conjunction with the phases given in *Table 4*. The contour interval is 1 electron/Å^2 and the zero contour is shown dotted

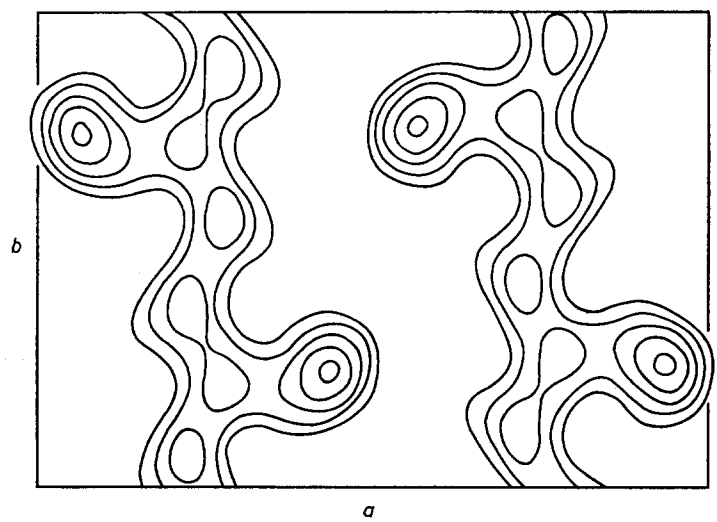

Figure 8—Electron density map of β-keratin using artificial sharpening to increase the resolution. The contour interval is 1 electron/Å^2 and the lowest contour corresponds to 2 electrons/Å^2

CONCLUSIONS

In an earlier study[8] it was suggested that the failure of the antiparallel chain pleated sheet structure to account satisfactorily for the observed X-ray diffraction pattern of β-keratin might be due to the occurrence of a mixture of parallel and antiparallel chain sheets in this material. This hypothesis provided a qualitative explanation for the overall weakness of the $hk0$ reflections with odd h. In the β-form of poly-L-alanine the equivalent reflections are completely absent and this has been shown to be due to disorder in sheet packing[3]. The present analysis shows that if a similar type of disorder is present in β-keratin the antiparallel chain pleated sheet structure accounts quantitatively for the observed diffraction pattern provided that the crystallites are assumed to be only 2·6 sheets thick on average. This assumption is borne out by the breadth of the 001 reflection which indicates an average crystal thickness in this direction of the order of only 22Å.

The average number of chains in a sheet was estimated in the present work to be 10·1 and so the average number of chains in a crystallite is estimated to be around 25. Each microfibril in native α-keratin is believed to contain about this number of α-helices[23,24] and this suggests that the chains in an individual β-crystallite probably all originate from the same microfibril. If this is so it implies that each microfibril contains equal numbers of oppositely directed chains.

A general weakness of the $hk0$ reflections with odd h has also been observed in the β-form of poly-γ-methyl-L-glutamate[25] and attributed to a parallel chain structure with occasional wrongly directed chains. This conclusion is in conflict with the evidence from infra-red studies[26], and in the light of the present investigation an antiparallel chain structure with disorder in sheet packing combined with limited crystal growth perpendicular to the plane of the pleated sheets would seem to be a more plausible explanation.

Whilst examples of the parallel chain pleated sheet may be found later, there do not seem to be any compelling reasons for assuming that extensive parallel chain pleated sheets are present in β-keratin, poly-γ-methyl-L-glutamate or as far as we are aware in any other fibrous protein or polypeptide that has so far been studied. Small numbers of parallel chains may of course occur in these materials as faults in otherwise antiparallel sheets.

APPENDIX 1

Inter-sheet disorder

The effect of random stacking of sheets as in the model proposed by Arnott, Dover and Elliott[3] for poly-L-alanine may be evaluated by means of the Multinominal Theorem. If, in a crystallite containing M sheets the probability that a sheet is correctly stacked to give orthogonal packing is $\frac{1}{2}$, the probability that m sheets are incorrectly stacked and $(M-m)$ correctly stacked is

$$\frac{M!}{(M-m)!m!}\left(\tfrac{1}{2}\right)^M \qquad (15)$$

If the transform of a correctly stacked sheet is $F_s(hk0)$ the transform of an incorrectly stacked sheet, displaced by $a/2$, will be

$$F_s(hk0)\exp(2\pi ih\times\tfrac{1}{2})=F_s(hk0)(-1)^h \tag{16}$$

The intensity from a crystallite with m incorrectly stacked sheets will be reduced for odd h by a factor

$$[(M-m)-m]^2/M^2=[(M-2m)/M]^2 \tag{17}$$

and on average the intensity will be reduced by a factor

$$\sum_{m=0}^{M}\left(\frac{M-2m}{M}\right)^2(\tfrac{1}{2})^M\frac{M!}{(M-m)!m!}=\frac{1}{M} \tag{18}$$

For reflections with even h the intensity is not affected by the random stacking.

APPENDIX 2

Intra-sheet disorder

Disorder in chain direction in a pleated sheet may be specified conveniently by a parameter p equal to the probability that a particular chain is correctly directed with respect to the preceding chain. The case $p=1$ corresponds to the ideal antiparallel and $p=0$ to the ideal parallel chain pleated sheet.

If we consider a sheet with N chains we may take the first chain as being correctly directed and label the remaining $(N-1)$ chains as either correctly directed in relation to the first (Type P) or incorrectly directed (Type Q). If there are r Q chains in a particular sheet they may occur either singly or in groups and the number of ways of dividing them into s sets each containing one or more chains is

$$\frac{(r-1)!}{(r-s)!(s-1)!}=\mathrm{C}(r-1,\ s-1),\ s\leqslant r \tag{19}$$

If there is a P chain at both ends of the sheet the number of ways in which s gaps between the $(N-r)$ P chains can be chosen is

$$\frac{(N-r-1)!}{(N-r-s-1)!s!}=\mathrm{C}(N-r-1,s),\ s\leqslant N-r-1 \tag{20}$$

and if the Nth chain is a Q chain

$$\frac{(N-r-1)!}{(N-r-s)!(s-1)!}=\mathrm{C}(N-r-1,s-1),\ s\leqslant N-r \tag{21}$$

Thus the probability of r Q chains in a sheet with N chains is

$$\sum_{s=1}^{s'} C(r-1, s-1)C(N-r-1, s)(1-p)^{2s}p^{N-2s-1} + \\ + \sum_{s=1}^{s''} C(r-1, s-1)C(N-r-1, s-1)(1-p)^{2s-1} \cdot p^{N-2s} \qquad (22)$$

where $s' \leqslant r$ and $\leqslant N-r-1$, $s'' \leqslant r$ and $\leqslant N-r$.

If the Fourier transform of the sheet is referred to an origin on the axis of the first chain the contribution of the nth chain will be, for P type chains,

$$F_{\alpha\delta} \exp [2\pi i h(n-1)\tfrac{1}{2}] \qquad (23)$$

if n is odd and

$$F^*_{\alpha\delta} \exp [2\pi i h(n-1)\tfrac{1}{2}] \qquad (24)$$

if n is even. If a chain is wrongly directed the effect will be to interchange these expressions.

For odd h the transform of a perfect sheet is

$$F_s = iB_{\alpha\delta}\left[\sum_{n \text{ odd}}(-1)^{n-1} - \sum_{n \text{ even}}(-1)^{n-1}\right] \qquad (25)$$

i.e.

$$F_s = iNB_{\alpha\delta} \qquad (26)$$

If a chain is wrongly directed its contribution will be of opposite sign and if the sheet contains r_o Q chains on odd sites and r_e Q chains on even sites

$$F_s = iB_{\alpha\delta}[(N/2 - r_o - r_e) + (N/2 - r_e - r_o)] \qquad (27)$$

i.e.

$$F_s = iB_{\alpha\delta}(N-2r) \qquad (28)$$

The effect on the observed intensity for odd h will therefore be to reduce the intensity by a factor γ equal to the mean value of $(N-2r)^2/N^2$.

From equation (22) we obtain

$$\gamma(p) = p^{N-1} + \sum_{r=1}^{N-1}\left(1-\frac{2r}{N}\right)^2\left[\sum_{s=1}^{s'} C(r-1, s-1)C(N-r-1, s)(1-p)^{2s}p^{N-2s-1} + \right. \\ \left. + \sum_{s=1}^{s''} C(r-1, s-1)C(N-r-1, s-1)(1-p)^{2s-1}p^{N-2s}\right] \qquad (29)$$

For even h the transform of a perfect sheet is from equations (23) and (24),

$$F_s = NA_{\alpha\delta} + iB_{\alpha\delta}\left[\sum_{n \text{ odd}} 1^{n-1} - \sum_{n \text{ even}} 1^{n-1}\right] \qquad (30)$$

i.e.

$$F_s = NA_{\alpha\delta} \qquad (31)$$

but for an imperfect sheet the two summations in equation (30) do not cancel and the difference between them is equal to

$$(\tfrac{1}{2}N - r_o + r_e) - (\tfrac{1}{2}N - r_e + r_o) = 2(r_e - r_o).$$

This is simply the excess of chains having a direction parallel to the first chain over those of opposite sense. The mean intensity for even h will therefore be greater than that for a perfect sheet by $B_{a\delta}^2$ multiplied by the mean value of $[2(r_e - r_o)]^2/N^2$ which may be shown by a similar argument to that presented earlier to be $\gamma(1-p)$.

Division of Protein Chemistry,
CSIRO,
Parkville (Melbourne),
Victoria 3052, Australia

(*Received March 1969*)

REFERENCES

[1] MARSH, R. E., COREY, R. B. and PAULING, L. *Biochim. Biophys. Acta* 1955, **16,** 1
[2] GEDDES, A. J., PARKER, K. D., ATKINS, E. D. T. and BEIGHTON, E. *J. Mol. Biol.* 1968, **32,** 343
[3] ARNOTT, S., DOVER, S. D. and ELLIOTT, A. *J. Mol. Biol.* 1967, **30,** 201
[4] PAULING, L. and COREY, R. B. *Proc. Nat. Acad. Sci. USA,* 1953, **39,** 253
[5] ASTBURY, W. T. and STREET, A. *Phil. Trans.* 1931, **A230,** 75
[6] ASTBURY, W. T. and WOODS, H. J. *Phil. Trans.* 1933, **A232,** 333
[7] MIYAZAWA, T. and BLOUT, E. R. *J. Amer. Chem. Soc.* 1961, **83,** 712
[8] FRASER, R. D. B. and MACRAE, T. P. *J. Mol. Biol.* 1962, **5,** 457
[9] BRADBURY, E. M. and ELLIOTT, A. *Polymer, Lond.* 1963, **4,** 47
[10] MARVIN, D. A., SPENCER, M., WILKINS, M. H. F. and HAMILTON, L. D. *J. Mol. Biol.* 1961, **3,** 547
[11] SUZUKI, E. *Spectrochim. Acta,* 1967, **23A,** 2303
[12] FRASER, R. D. B. and SUZUKI, E. *Spectrochim. Acta,* 1965, **21,** 615
[13] FRASER, R. D. and SUZUKI, E. *Analyt. Chem.* 1966, **38,** 1770
[14] ARNOTT, S. and WONACOTT, A. J. *Polymer, Lond.* 1966. **7,** 157
[15] SCOTT, R. A. and SCHERAGA, H. A. *J. Chem. Phys.* 1966, **45,** 2091
[16] OOI, T., SCOTT, R. A., VANDERKOOI, G. and SCHERAGA, H. A. *J. Chem. Phys.* 1967, **46,** 4410
[17] LEACH, S. J., NÉMETHY, G. and SCHERAGA, H. A. *Biopolymers,* 1966, **4,** 369
[18] PARRY, D. A. D. and SUZUKI, E. *Biopolymers* 1969, **7,** 189
[19] ARNOTT, S. *Polymer, Lond.* 1965, **6,** 478
[20] HAMILTON, W. C. *Acta Cryst.* 1965, **18,** 502
[21] MIYAZAWA, T. *J. Chem. Phys.* 1960, **32,** 1647
[22] FRASER, R. D. B. and SUZUKI, E. *Spectrochim. Acta* (in press)
[23] FRASER, R. D. B., MACRAE, T. P. and MILLER, A. *J. Mol. Biol.* 1965, **14,** 432
[24] BENDIT, E. G. *Text. Res. J* 1968, **38,** 15
[25] VAINSHTEIN, B. K. and TATARINOVA, L. I. *Conformation of Biopolymers,* Vol. 2, G. N. Ramachandran (ed.), Academic Press, 1967, p 569
[26] BAMFORD, C. H., ELLIOTT, A. and HANBY, W. E. *Synthetic Polypeptides,* Academic Press, 1956